


Predictable Gate-Field Control of Spin in Altermagnets with Spin-Layer Coupling

Run-Wu Zhang,^{1,2,*} Chaoxi Cui,^{1,*} Runze Li,¹ Jingyi Duan,¹ Lei Li,¹ Zhi-Ming Yu^{①,1,2,†} and Yugui Yao^{1,2,‡}

¹Key Lab of Advanced Optoelectronic Quantum Architecture and Measurement (MOE),
Beijing Key Lab of Nanophotonics & Ultrafine Optoelectronic Systems, and School of Physics,
Beijing Institute of Technology, Beijing 100081, China

²International Center for Quantum Materials, Beijing Institute of Technology, Zhuhai, 519000, China

 (Received 11 July 2023; revised 22 January 2024; accepted 6 June 2024; published 1 August 2024)

Spintronics, a technology harnessing electron spin for information transmission, offers a promising avenue to surpass the limitations of conventional electronic devices. While the spin directly interacts with the magnetic field, its control through the electric field is generally more practical, and has become a focal point in the field. Here, we propose a mechanism to realize static and almost uniform effective magnetic field by gate-electric field. Our method employs two-dimensional altermagnets with valley-mediated spin-layer coupling (SLC), in which electronic states display valley-contrasted spin and layer polarization. For the low-energy valley electrons, a uniform gate field is approximately identical to a uniform magnetic field, leading to predictable control of spin. Through symmetry analysis and *ab initio* calculations, we predict altermagnetic monolayer $\text{Ca}(\text{CoN})_2$ and its family materials as potential candidates hosting SLC. We show that an almost uniform magnetic field (B_z) indeed is generated by gate field (E_z) in $\text{Ca}(\text{CoN})_2$ with $B_z \propto E_z$ in a wide range, and B_z reaches as high as about 10^3 T when $E_z = 0.2$ eV/Å. Furthermore, owing to the clean band structure and SLC, one can achieve perfect and switchable spin and valley currents and significant tunneling magnetoresistance in $\text{Ca}(\text{CoN})_2$ solely using the gate field. Our work provides new opportunities to generate predictable control of spin and design spintronic devices that can be controlled by purely electric means.

DOI: [10.1103/PhysRevLett.133.056401](https://doi.org/10.1103/PhysRevLett.133.056401)

Introduction—The discovery of various spin-dependent transport phenomena [1–13] has led to the emergence of the field of spintronics, which has generated extensive interest in both fundamental research and application design [14–30]. For advanced spintronics devices, an efficient and precise control of spin is required. Since spin is a type of angular momentum, a magnetic field is the most natural way to control it. Under a uniform magnetic field \mathbf{B} , the energy of an electron with spin angular momentum s will be shifted by $\Delta \propto -\mathbf{B} \cdot s$ [31,32]. According to this Zeeman effect, the behavior of spin under a B field can be easily predicted, indicating that one can use a B field to precisely control spin. However, magnetic control of spin is not favored in application.

Various schemes are proposed to control spin via non-magnetic methods. Since the spin-orbit coupling (SOC) effect couples an electron's motion (or momentum) to spin, most of the current schemes use SOC to generate an effective B field by electric means [33–36]. In the view of symmetry, the addition of external fields may reduce the symmetry of the systems and then may lead to indirect control of spin via certain mechanisms in the systems both with and without

SOC [37–47]. For example, an external electric field and interface engineering, which break spacetime-inversion (PT) symmetry, generally can lead to net spin polarization [41,42]. However, the effective B field induced by these schemes generally has a strong dependence on momentum \mathbf{k} and is not uniform even for the low-energy electrons. Moreover, in practice using only a gate electric field to induce an effective uniform magnetic field would be ideal [48–55].

The gate field is directly coupled to the layer degree of freedom. For a two-dimensional (2D) material with multiple atomic layers, a perpendicular gate field (E_z) can create a layer-dependent electrostatic potential. Then, when the band electrons with opposite spin polarization have finite and opposite layer polarization ($\pm P_l$), an emergent spin-layer coupling (SLC) occurs. With SLC, the gate field can produce an energy shift of $\Delta \propto -E_z P_l$ for the electrons with opposite spins, similar to the Zeeman effect. Particularly, the SLC scheme works for the systems both with and without the SOC effect. However, to generate a uniform B field via SLC, both spin and layer polarization of *all* the low-energy electronic states should be the same or opposite. This means that generic interlayer antiferromagnets like bilayer CrI_3 cannot accomplish the task, as their low-energy electrons are distributed in different regions of the Brillouin zone (BZ) having completely different spin and layer polarization.

*These authors contributed equally to this work.

†Contact author: zhiming_yu@bit.edu.cn

‡Contact author: ygyao@bit.edu.cn

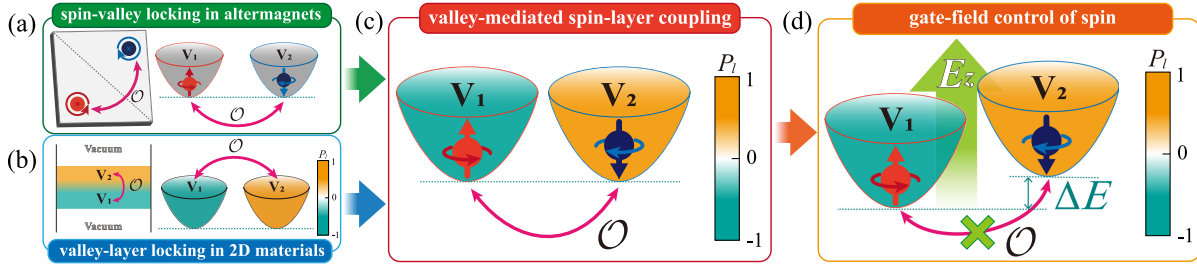


FIG. 1. Illustration of the mechanism of valley-mediated SLC and the gate-field control of spin. (a) A generic altermagnet with two valleys V_1 and V_2 features intrinsic spin-valley locking, which is protected by certain (magnetic) crystalline symmetry \mathcal{O} rather than time-reversal symmetry \mathcal{T} . (b) Meanwhile, a 2D valleytronic material may host \mathcal{O} -protected valley-layer locking, where the two valley states have opposite layer polarization (P_l). (c) The combination of spin-valley and valley-layer locking leads to a novel spin-valley-layer coupling: valley-mediated SLC in 2D altermagnets. (d) This effect enables an intuitive, predictable, and precise control of the spin polarization by electric gate field.

Besides, for the famous spintronics (valleytronics) materials, transitional metal dichalcogenides (TMD), their low-energy electrons are localized at the K or K' valley and then share similar or opposite physical properties. But since the bilayer TMD has time-reversal symmetry [56,57], the gate field *alone* may produce finite spin polarization in each valley but cannot generate net spin polarization. Therefore, for further development of spintronics, it is crucial to find a magnetic counterpart of the TMDs, which not only has abundant coupled physics but also permits a predictable control of spin polarization via gate field alone.

Here, we address this task by proposing a novel type of spin-valley-layer coupling, valley-mediated SLC, and predicting ideal material candidates: monolayer $\text{Ca}(\text{CoN})_2$ and its family materials. Here, the ideal means that the band structure is clean and the SLC effect is significant. We show that the valley-mediated SLC can naturally appear in the 2D valleytronics materials with altermagnetic ordering and valley-layer coupling, as illustrated in Fig. 1. Via *ab initio* calculations on $\text{Ca}(\text{CoN})_2$, we find that an almost uniform effective magnetic field indeed is generated by gate field, and its strength reaches $\sim 10^3$ T for $E_z = 0.2$ eV/Å. Moreover, several interesting phenomena associated with SLC are revealed, such as a new design scheme for realizing a giant tunneling magnetoresistance (TMR)-like device without a heterojunction structure. Our work thus opens a new research direction for the field of spintronics.

Valley-mediated SLC—Since our target is generating spin polarization through the gate field alone, the systems studied here should be spin neutral but break time-reversal symmetry (\mathcal{T}). We also require the low-energy electrons to have similar or opposite polarizations. These requirements naturally point to the 2D valleytronics materials with antiferromagnetic or altermagnetic (AM) ordering. However, the bands in antiferromagnetic materials are at least doubly degenerate, making the polarization ill defined.

Thus, we consider a generic AM material, where the low-energy bands around each valley are not degenerate. Owing to the altermagnetism, the valleys must come in pairs with

opposite spin polarization, leading to intrinsic spin-valley locking [43,45], as shown in Fig. 1(a). Furthermore, certain 2D valleytronics materials can host valley-layer coupling [58], where the electronic states in different valleys have opposite layer polarization [see Fig. 1(b)]. By combining both effects, the electronic states with opposite spin polarization (in different valleys) will exhibit opposite layer polarization, leading to the valley-mediated SLC [see Fig. 1(c)]. With this SLC effect, a uniform electric field can act as an (almost) uniform magnetic field to influence the spin-polarized bands, enabling precise control of the spin by gate field [see Fig. 1(d)].

Symmetry requirements—We then analyze the symmetry conditions for the valley-mediated SLC. For simplicity, we consider a 2D collinear AM system with only two valleys labeled as V_1 and V_2 (see Fig. 1). We also assume that the Néel vector of the system points out of the plane; in such case, the directions of the spin polarization of the valley electrons for the systems without SOC must be along the $\pm z$ direction (as an infinitesimal SOC effect can fix the spin polarization of systems to these directions), while for the systems with strong SOC, they may or may not be along the $\pm z$ direction. For consistency of discussion, we further require the spin polarization of the valley electrons to be approximately along the $\pm z$ direction in the SOC systems.

For each Bloch state $|\psi(\mathbf{k})\rangle$, we can define a spin (layer) polarization $P_{s(l)} = \langle \psi(\mathbf{k}) | \hat{P}_{s(l)} | \psi(\mathbf{k}) \rangle$ with $\hat{P}_s \equiv \hat{s}_z$ ($\hat{P}_l \equiv \hat{r}_z$) denoting the z component of the spin (position) operator. $P_s > 0$ ($P_s < 0$) and $P_l > 0$ ($P_l < 0$) indicate that the state has more weight distributed in the spin-up (spin-down) and top (bottom) layer, respectively. Notice that $P_{s(l)}$ and the spin (layer) polarization of the magnetic atoms are two completely different concepts, which are respectively defined in \mathbf{k} space and real space. Therefore, it is not reasonable to infer $P_{s(l)}$ from the magnetic configuration of systems.

To realize the valley-mediated SLC, the following symmetry requirements must be satisfied: (i) Symmetries that guarantee vanishing spin or layer polarization at $V_{1(2)}$ should be broken, such as horizontal mirror \mathcal{M}_z , which

makes $P_l = 0$ for all the bands and (ii) we can divide the symmetries of the AM system into two parts, \mathcal{R} and \mathcal{O} ; V_1 and V_2 are invariant (interchanged) under the operators in \mathcal{R} (\mathcal{O}), as follows:

$$\mathcal{R}V_{1(2)} = V_{1(2)}, \quad \mathcal{O}V_{1(2)} = V_{2(1)}. \quad (1)$$

To achieve valley-contrasted spin and layer polarization, any operator in \mathcal{R} must maintain both spin and layer polarizations for each valley:

$$\mathcal{R}P_{l(s)}(V_i)\mathcal{R}^{-1} = P_{l(s)}(V_i), \quad (2)$$

with $i = 1, 2$. Meanwhile, any operator in \mathcal{O} reverses the polarizations:

$$\mathcal{O}P_{l(s)}(V_{1/2})\mathcal{O}^{-1} = -P_{l(s)}(V_{2/1}). \quad (3)$$

This indicates that the gate field should break \mathcal{O} .

These two requirements apply to the systems with and without SOC, the symmetry of which are described by magnetic groups and spin groups, respectively. For SLC, the main difference between the magnetic group [59] and the spin group [60–62] is the constraints they imposed on spin polarization. Notice that, we have assumed that the spin polarization of the valley electrons for the systems with and without SOC are the same, i.e., pointing along the $\pm z$ direction. Thus, for the magnetic systems discussed here, it is enough and convenient to use the magnetic groups rather than the complicated spin groups to analyze the SLC in the systems without SOC [63]. We conducted a search through all 528 magnetic layer groups (MLGs) to identify those that may host valley-mediated SLC. Our findings are summarized in Table S1 of the Supplemental Material [63], which provides a systematic and specific guide for identifying material candidates.

Candidate materials—In addition to developing design principles, it is equivalently important to identify candidate materials. Here, we demonstrate that the family of monolayer decorated transition metal nitride $A(BN)_2$ ($A = \text{Mg, Ca, Zn}$ and $B = \text{Mn, Fe, Co}$) materials are the potential candidates with valley-mediated SLC; among them the monolayer $\text{Ca}(\text{CoN})_2$ is the most representative. We focus on the monolayer $\text{Ca}(\text{CoN})_2$ in the main text. The properties of the other candidates can be found in the Supplemental Material [63].

The monolayer $\text{Ca}(\text{CoN})_2$ has a square lattice structure with optimized lattice constant $a = b = 3.55 \text{ \AA}$, consisting of five atomic layers in the sequence of Co-N-Ca-N-Co [see Figs. 2(a) and 2(b)]. The top (bottom) Co and N atoms are almost in the same plane. Remarkably, the separation between the top and bottom Co-N layers is about 3.9 \AA , which is as large as the typical interlayer spacing of van der Waals heterostructures. We confirm that the ground state of monolayer $\text{Ca}(\text{CoN})_2$ exhibits an AM configuration [63], as illustrated in Fig. 2(c), and belongs to MLG 59.5.414, which is exactly a target MLG candidate. The magnetic

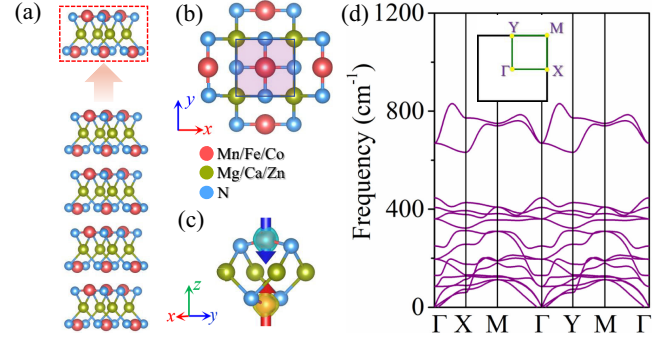


FIG. 2. (a) Schematic showing the process of stripping monolayer candidates (red dashed area) from the bulk. (b) Top view of the crystal structure of monolayer $A(BN)_2$. (c) Spatial spin-density distribution of monolayer $\text{Ca}(\text{CoN})_2$, showing the magnetic moments are mainly localized around the top and bottom Co atoms with opposite directions. (d) Phonon spectrum of the monolayer $\text{Ca}(\text{CoN})_2$.

moments are mainly on the Co sites with a magnitude of $\sim 3\mu_B$, and the Néel vector is along the z axis. The monolayer $\text{Ca}(\text{CoN})_2$ is also dynamically stable [see Fig. 2(d)] and features thermal stability up to 300 K [63].

According to our symmetry analysis [63], the monolayer $\text{Ca}(\text{CoN})_2$ will exhibit valley-mediated SLC as long as it has two valleys at the X and Y points. In fact, these two valleys are connected by \mathcal{TS}_{4z} symmetry (with $S_{4z} = C_{4z}\mathcal{P}$), which interchanges both spin and layer polarizations (P_s and P_l) of the two valleys. Since the monolayer $\text{Ca}(\text{CoN})_2$ has negligible SOC effect, it can be considered as an AM without SOC. The band structure of the monolayer $\text{Ca}(\text{CoN})_2$ without SOC is shown in Fig. 3(a), where two valleys for both the conduction and valence bands at the X and Y points are observed. Therefore, we can conclude that the valley states must feature valley-contrasted spin and layer polarization. By analyzing the spin projection of the valley states, we find that both the conduction and valence bands residing at the X valley are completely composed of spin-up, while those at the Y valley only contain spin-down [see Fig. 3(a)]. Additionally, the conduction band at the X (Y) valley is mainly distributed in the top (bottom) Co-N layer, whereas the valence band at the X (Y) valley is mainly distributed in the bottom (top) Co-N layer [see Fig. 3(b)]. We have checked that the band dispersion and the two polarizations of the two valleys remain unchanged when SOC is included, consistent with the above analysis [63]. These results explicitly demonstrate the existence of the valley-mediated SLC.

Gate-field control of spin—Owing to SLC, one can easily predict the behavior of the spin states of the monolayer $\text{Ca}(\text{CoN})_2$ under E_z . For the conduction band, the gate field ($E_z > 0$) pushes up the X valley with spin-up and pulls down the Y valley with spin-down, behaving like a magnetic field pointing along the z direction with $B_c^{\text{eff}} > 0$. For the valence band, the spin splitting is opposite because the layer polarization of the spin states around X and Y valleys are reversed [see Fig. 3(b)], leading to an

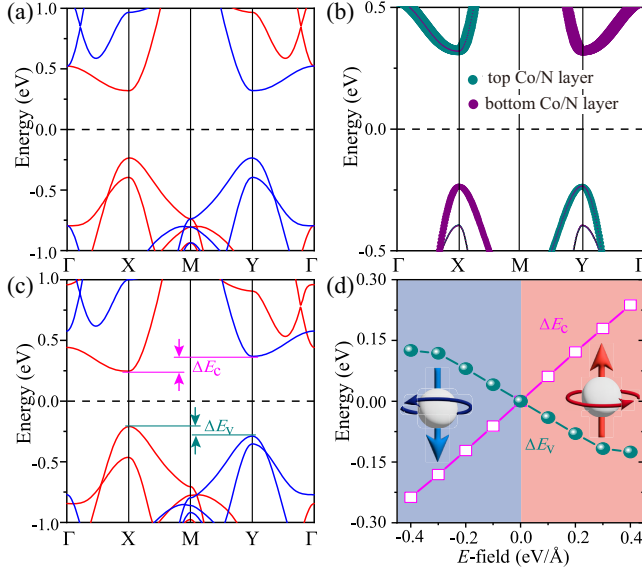


FIG. 3. (a) Band structure of monolayer $\text{Ca}(\text{CoN})_2$ in the AM configuration without SOC. The red color denotes the spin-up channel, and the blue color stands for the spin-down channel, respectively. (b) Orbital-projected band structures without SOC, showing the low-energy bands are mainly contributed by Co and N atoms. (c) Band structure of monolayer $\text{Ca}(\text{CoN})_2$ under a gate field of $E_z = 0.2 \text{ eV/\AA}$. (d) Spin (valley) splitting for VBM (ΔE_v) and CBM (ΔE_c) [indicated in (c)] versus E_z .

effective magnetic field of $B_v^{\text{eff}} < 0$. Figure 3(c) shows the calculated band structure of the monolayer $\text{Ca}(\text{CoN})_2$ with an experimentally achievable gate field of $E_z = 0.2 \text{ eV/\AA}$ [74]. The results are consistent with our expectations. Moreover, the induced B field in monolayer $\text{Ca}(\text{CoN})_2$ has the following distinctive features.

First, the conduction (valence) states around the X (Y) valley have almost the same energy shift [63], indicating that the gate field induces a static and uniform effective B field. To the best of our knowledge, the uniform effective B field has not been reported before and cannot generally be generated by schemes other than the SLC scheme.

Second, the spin splitting of the conduction band minimum (CBM) and valence band maximum (VBM) is significant, respectively reaching up to 123 meV and 78 meV for $E_z = 0.2 \text{ eV/\AA}$ [see Figs. 3(c) and 3(d)].

The strength of the induced effective magnetic field may be approximately expressed as

$$B_{c(v)}^{\text{eff}} \equiv \frac{\Delta E_{c(v)}}{g_s s_z}, \quad (4)$$

where ΔE_c (ΔE_v) is the energy splitting for CBM (VBM), $s_z = 1/2$, and g_s is the effective g factor which here is assumed to be 2. From Eq. (4), one knows that for the conduction (valence) band, a gate field of $E_z = 0.2 \text{ eV/\AA}$ produces a B field as large as 1062 T (−673 T).

Third, we also calculate the spin splitting as a function of E_z , and the result is shown in Fig. 3(d), which clearly shows

that a continuous, wide-range, and switchable control of spin (valley) polarization is achieved. Particularly, a linear relationship between the $B_{c(v)}^{\text{eff}}$ and E_z can be observed in a wide range. Approximately, we have $B_{c(v)}^{\text{eff}} = \chi_{c(v)} E_z$ with $\chi_c = 5.15 \times 10^3 \text{ T\AA/V}$ and $\chi_v = -2.71 \times 10^3 \text{ T\AA/V}$. All these features are highly advantageous for the application of the gate-field control of spin.

Effective model for valley-mediated SLC—Another advantage of the valley-mediated SLC is that we can establish a low-energy effective Hamiltonian to describe it. The magnetic point group of the X and Y valleys is $m'm'2$ for the monolayer $\text{Ca}(\text{CoN})_2$. The band representation of the CBM (φ_c^X) and VBM (φ_v^X) at the X valley of the monolayer $\text{Ca}(\text{CoN})_2$ with SOC is ${}^2\bar{E}$ and ${}^1\bar{E}$ respectively, while that of the CBM (φ_c^Y) and VBM (φ_v^Y) at the Y valley is ${}^1\bar{E}$ and ${}^2\bar{E}$. Using the four states $\{\varphi_c^X, \varphi_v^X, \varphi_c^Y, \varphi_v^Y\}$ as the basis, the $k \cdot p$ effective model can be expressed as

$$\mathcal{H} = \Lambda \tau_z + v_1(k_x \tau_x + k_y \tau_y) + v_2(k_x \tau_x - k_y \tau_y) \sigma_z, \quad (5)$$

where $\Lambda = 0.281 \text{ eV}$ is the half of the band gap, $v_1 = 0.760 \text{ eV/\AA}$, and $v_2 = 0.748 \text{ eV/\AA}$ ($v_1 = v_2$ when the SOC effect is ignored.) Both σ and τ are Pauli matrices that act on the valley space and the basis of $\{\varphi_c^V, \varphi_v^V\}$ with $V = X$ and Y , respectively. Since the basis $\{\varphi_c^V, \varphi_v^V\}$ has opposite layer polarization, τ can also be regarded as acting on the layer space. Similarly, σ can also be considered to operate in the spin space, as the low-energy states at the X (Y) valley are spin-up (spin-down) electrons. Therefore, the physics of the SLC is solely encoded in the last term of Eq. (5) which pairs τ with σ . With the concept of the effective magnetic field, the main influence of the gate field on the low-energy bands of monolayer $\text{Ca}(\text{CoN})_2$ can be written as

$$\mathcal{H}_E = -s_z g_s \text{diag}(B_c^{\text{eff}}, B_v^{\text{eff}}, -B_c^{\text{eff}}, -B_v^{\text{eff}}). \quad (6)$$

Discussions—Owing to valley-mediated SLC, the monolayer $\text{Ca}(\text{CoN})_2$ is an ideal material for realizing various spintronics devices with great advantages in controllability, significance, and convenience. On doping the monolayer $\text{Ca}(\text{CoN})_2$ with either electrons or holes, and subjecting it to a gate field, the system exhibits a significant spin polarization, for which the polarized direction can be easily switched by reversing the gate field. Thus, the monolayer $\text{Ca}(\text{CoN})_2$ is a suitable platform for generating a current with perfect and switchable spin polarization.

The TMR device, an important spintronics device, generally requires a heterojunction structure and is controlled by a magnetic field. However, the gate-field control of spin in monolayer $\text{Ca}(\text{CoN})_2$ suggests a new paradigm for achieving a TMR-like device without both a heterojunction structure and magnetic field, which would significantly simplify the experimental procedures. As illustrated in Fig. 4, the device is constructed by the monolayer $\text{Ca}(\text{CoN})_2$ alone and is divided into three regions by gate field. For parallel (antiparallel) configuration, the gate field at

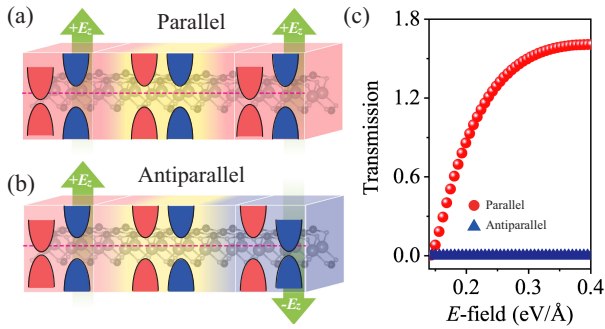


FIG. 4. Schematic of novel TMR-like device based on monolayer $\text{Ca}(\text{CoN})_2$. (a),(b) Parallel and antiparallel configurations of the TMR-like device. (c) Total transmission as a function of E_z for the $\text{Ca}(\text{CoN})_2$ tunnel junction in parallel and antiparallel configurations. The calculation details are shown in the Supplemental Material [63].

the left and right regions is the same (opposite). With a suitable Fermi level, the middle region is still insulated while the other regions become doped. In a parallel configuration, the matched conduction channels between the left and right regions would result in a low-resistance state. In contrast, in an antiparallel configuration, electrons moving from left to right must switch spin, valley, and layer indexes, i.e., changing from spin-up, X valley, and top layer to spin-down, Y valley, and bottom layer, making the tunneling resistance of the system extremely high. For conventional TMR devices, only the spin index changes in the antiparallel configuration. Therefore, compared with them, our design should exhibit stronger suppression in the antiparallel configuration, and then feature a more pronounced TMR effect. We present the calculated overall transmission for both parallel and antiparallel configurations in Fig. 4(c), which clearly demonstrates our analysis.

Besides, the unique band structure of the monolayer $\text{Ca}(\text{CoN})_2$ leads to many intriguing and adjustable optical properties. From Eq. (5), we find that the monolayer $\text{Ca}(\text{CoN})_2$ exhibits valley- and spin-contrasted elliptical dichroism [63]. Then, the opposing layer polarization of valence and conduction bands at each valley will generate spin-resolved interlayer excitons [58] and layer photogalvanic effects [75] under left or right elliptically polarized light, as optically excited electrons and holes are localized in different layers. Furthermore, one can use the gate field to effectively modulate the interlayer excitons and photogalvanic effects.

Acknowledgments—This work is supported by the National Key R&D Program of China (Grant No. 2020YFA0308800), the National Natural Science Foundation of China (Grants No. 12234003, No. 12004035, No. 12304188, No. 12321004, No. 12347214), and the Beijing Institute of Technology Research Fund Program for Young Scholars.

- [1] M. Julliere, *Phys. Lett.* **54A**, 225 (1975).
- [2] M. N. Baibich, J. M. Broto, A. Fert, F. Nguyen Van Dau, F. Petroff, P. Etienne, G. Creuzet, A. Friederich, and J. Chazelas, *Phys. Rev. Lett.* **61**, 2472 (1988).
- [3] G. Binasch, P. Grünberg, F. Saurenbach, and W. Zinn, *Phys. Rev. B* **39**, 4828 (1989).
- [4] J. S. Moodera, L. R. Kinder, T. M. Wong, and R. Meservey, *Phys. Rev. Lett.* **74**, 3273 (1995).
- [5] A. Milner, A. Gerber, B. Groisman, M. Karpovsky, and A. Gladkikh, *Phys. Rev. Lett.* **76**, 475 (1996).
- [6] E. Y. Tsymbal, O. N. Mryasov, and P. R. LeClair, *J. Phys. Condens. Matter* **15**, R109 (2003).
- [7] S. Zhang and Z. Li, *Phys. Rev. Lett.* **93**, 127204 (2004).
- [8] P. Merodio, A. Kalitsov, H. Béa, V. Baltz, and M. Chshiev, *Appl. Phys. Lett.* **105**, 122403 (2014).
- [9] T. Jungwirth, J. Wunderlich, V. Novák, K. Olejník, B. L. Gallagher, R. P. Campion, K. W. Edmonds, A. W. Rushforth, A. J. Ferguson, and P. Němec, *Rev. Mod. Phys.* **86**, 855 (2014).
- [10] P. Wadley, B. Howells, J. Železný, C. Andrews, V. Hills, R. P. Campion, V. Novák, K. Olejník, F. Maccherozzi, S. Dhesi *et al.*, *Science* **351**, 587 (2016).
- [11] S. Y. Bodnar, L. Šmejkal, I. Turek, T. Jungwirth, O. Gomonay, J. Sinova, A. Sapozhnik, H.-J. Elmers, M. Kläui, and M. Jourdan, *Nat. Commun.* **9**, 348 (2018).
- [12] J. Železný, P. Wadley, K. Olejník, A. Hoffmann, and H. Ohno, *Nat. Phys.* **14**, 220 (2018).
- [13] D.-F. Shao, S.-H. Zhang, M. Li, C.-B. Eom, and E. Y. Tsymbal, *Nat. Commun.* **12**, 7061 (2021).
- [14] I. Žutić, J. Fabian, and S. D. Sarma, *Rev. Mod. Phys.* **76**, 323 (2004).
- [15] A. Fert, *Rev. Mod. Phys.* **80**, 1517 (2008).
- [16] B. Dieny, I. L. Prejbeanu, K. Garello, P. Gambardella, P. Freitas, R. Lehdorff, W. Raberg, U. Ebels, S. O. Demokritov, J. Akerman *et al.*, *National electronics review* **3**, 446 (2020).
- [17] S. K. Kim, G. S. Beach, K.-J. Lee, T. Ono, T. Rasing, and H. Yang, *Nat. Mater.* **21**, 24 (2022).
- [18] J. Han, R. Cheng, L. Liu, H. Ohno, and S. Fukami, *Nat. Mater.* **22**, 684 (2023).
- [19] L. Šmejkal, A. B. Hellenes, R. González-Hernández, J. Sinova, and T. Jungwirth, *Phys. Rev. X* **12**, 011028 (2022).
- [20] L. Šmejkal, J. Sinova, and T. Jungwirth, *Phys. Rev. X* **12**, 031042 (2022).
- [21] L.-D. Yuan, Z. Wang, J.-W. Luo, E. I. Rashba, and A. Zunger, *Phys. Rev. B* **102**, 014422 (2020).
- [22] L.-D. Yuan, Z. Wang, J.-W. Luo, and A. Zunger, *Phys. Rev. Mater.* **5**, 014409 (2021).
- [23] S. Hayami, Y. Yanagi, and H. Kusunose, *J. Phys. Soc. Jpn.* **88**, 123702 (2019).
- [24] S. A. Egorov, D. B. Litvin, and R. A. Evarestov, *J. Phys. Chem. C* **125**, 16147 (2021).
- [25] S. A. Egorov, D. B. Litvin, A. V. Bandura, and R. A. Evarestov, *J. Phys. Chem. C* **126**, 5362 (2022).
- [26] Z. Feng, X. Zhou, L. Šmejkal, L. Wu, Z. Zhu, H. Guo, R. González-Hernández, X. Wang, H. Yan, P. Qin *et al.*, *Nat. Electron.* **5**, 735 (2022).
- [27] P. Liu, J. Li, J. Han, X. Wan, and Q. Liu, *Phys. Rev. X* **12**, 021016 (2022).

- [28] W. Chen, M. Gu, J. Li, P. Wang, and Q. Liu, *Phys. Rev. Lett.* **129**, 276601 (2022).
- [29] X.-Y. Hou, H.-C. Yang, Z.-X. Liu, P.-J. Guo, and Z.-Y. Lu, *Phys. Rev. B* **107**, L161109 (2023).
- [30] P.-J. Guo, Z.-X. Liu, and Z.-Y. Lu, *npj Comput. Mater.* **9**, 70 (2023).
- [31] S. Wolf, D. Awschalom, R. Buhrman, J. Daughton, v. S. von Molnár, M. Roukes, A. Y. Chtchelkanova, and D. Treger, *Science* **294**, 1488 (2001).
- [32] T. Schäpers, *MRS Bull.* **42**, 615 (2017).
- [33] A. Manchon, H. C. Koo, J. Nitta, S. M. Frolov, and R. A. Duine, *Nat. Mater.* **14**, 871 (2015).
- [34] L.-P. Yang and C.-P. Sun, *Eur. Phys. J. B* **88**, 35 (2015).
- [35] A. V. Larionov and L. E. Golub, *Phys. Rev. B* **78**, 033302 (2008).
- [36] X. Qian, J. Liu, L. Fu, and J. Li, *Science* **346**, 1344 (2014).
- [37] H. Yuan, M. S. Bahramy, K. Morimoto, S. Wu, K. Nomura, B.-J. Yang, H. Shimotani, R. Suzuki, M. Toh, C. Kloc *et al.*, *Nat. Phys.* **9**, 563 (2013).
- [38] H. Yuan, X. Wang, B. Lian, H. Zhang, X. Fang, B. Shen, G. Xu, Y. Xu, S.-C. Zhang, H. Y. Hwang *et al.*, *Nat. Nanotechnol.* **9**, 851 (2014).
- [39] K. Liu, W. Luo, J. Ji, P. Barone, S. Picozzi, and H. Xiang, *Nat. Commun.* **10**, 5144 (2019).
- [40] H. J. Zhao, X. Liu, Y. Wang, Y. Yang, L. Bellaiche, and Y. Ma, *Phys. Rev. Lett.* **129**, 187602 (2022).
- [41] S.-J. Gong, C. Gong, Y.-Y. Sun, W.-Y. Tong, C.-G. Duan, J.-H. Chu, and X. Zhang, *Proc. Natl. Acad. Sci. U.S.A.* **115**, 8511 (2018).
- [42] V. P. Amin, J. Zemen, and M. D. Stiles, *Phys. Rev. Lett.* **121**, 136805 (2018).
- [43] R. González-Hernández, L. Šmejkal, K. Výborný, Y. Yahagi, J. Sinova, T. Jungwirth, and J. Železný, *Phys. Rev. Lett.* **126**, 127701 (2021).
- [44] L. Šmejkal, J. Sinova, and T. Jungwirth, *Phys. Rev. X* **12**, 040501 (2022).
- [45] H.-Y. Ma, M. Hu, N. Li, J. Liu, W. Yao, J.-F. Jia, and J. Liu, *Nat. Commun.* **12**, 2846 (2021).
- [46] D.-F. Shao, Y.-Y. Jiang, J. Ding, S.-H. Zhang, Z.-A. Wang, R.-C. Xiao, G. Gurung, W. J. Lu, Y. P. Sun, and E. Y. Tsymbal, *Phys. Rev. Lett.* **130**, 216702 (2023).
- [47] Y.-Y. Jiang, Z.-A. Wang, K. Samanta, S.-H. Zhang, R.-C. Xiao, W. Lu, Y. Sun, E. Y. Tsymbal, and D.-F. Shao, *arXiv:2309.02634*.
- [48] H. Ohno, a. D. Chiba, a. F. Matsukura, T. Omiya, E. Abe, T. Dietl, Y. Ohno, and K. Ohtani, *Nature (London)* **408**, 944 (2000).
- [49] S. Sahoo, T. Kontos, J. Furer, C. Hoffmann, M. Gräber, A. Cottet, and C. Schönenberger, *Nat. Phys.* **1**, 99 (2005).
- [50] P. Rovillain, R. De Sousa, Y. Gallais, A. Sacuto, M. Méasson, D. Colson, A. Forget, M. Bibes, A. Barthélémy, and M. Cazayous, *Nat. Mater.* **9**, 975 (2010).
- [51] S. H. Chun, Y. S. Chai, B.-G. Jeon, H. J. Kim, Y. S. Oh, I. Kim, H. Kim, B. J. Jeon, S. Y. Haam, J.-Y. Park *et al.*, *Phys. Rev. Lett.* **108**, 177201 (2012).
- [52] S. Gong, H. Ding, W. Zhu, C. Duan, Z. Zhu, and J. Chu, *Sci. China Phys. Mech. Astron.* **56**, 232 (2013).
- [53] J. Heron, J. Bosse, Q. He, Y. Gao, M. Trassin, L. Ye, J. Clarkson, C. Wang, J. Liu, S. Salahuddin *et al.*, *Nature (London)* **516**, 370 (2014).
- [54] P. Noël, F. Trier, L. M. Vicente Arche, J. Bréhin, D. C. Vaz, V. Garcia, S. Fusil, A. Barthélémy, L. Vila, M. Bibes *et al.*, *Nature (London)* **580**, 483 (2020).
- [55] J. Ingla-Aynés, F. Herling, J. Fabian, L. E. Hueso, and F. Casanova, *Phys. Rev. Lett.* **127**, 047202 (2021).
- [56] A. M. Jones, H. Yu, J. S. Ross, P. Klement, N. J. Ghimire, J. Yan, D. G. Mandrus, W. Yao, and X. Xu, *Nat. Phys.* **10**, 130 (2014).
- [57] C. Jiang, F. Liu, J. Cuadra, Z. Huang, K. Li, A. Rasmita, A. Srivastava, Z. Liu, and W.-B. Gao, *Nat. Commun.* **8**, 802 (2017).
- [58] Z.-M. Yu, S. Guan, X.-L. Sheng, W. Gao, and S. A. Yang, *Phys. Rev. Lett.* **124**, 037701 (2020).
- [59] Z. Zhang, W. Wu, G.-B. Liu, Z.-M. Yu, S. A. Yang, and Y. Yao, *Phys. Rev. B* **107**, 075405 (2023).
- [60] Y. Jiang, Z. Song, T. Zhu, Z. Fang, H. Weng, Z.-X. Liu, J. Yang, and C. Fang, *arXiv:2307.10371* [*Phys. Rev. X* (to be published)].
- [61] Z. Xiao, J. Zhao, Y. Li, R. Shindou, and Z.-D. Song, *arXiv:2307.10364* [*Phys. Rev. X* (to be published)].
- [62] J. Ren, X. Chen, Y. Zhu, Y. Yu, A. Zhang, J. Li, C. Li, and Q. Liu, *arXiv:2307.10369* [*Phys. Rev. X* (to be published)].
- [63] See Supplemental Material at <http://link.aps.org/supplemental/10.1103/PhysRevLett.133.056401> for a detailed description of computational methods, symmetry analysis, supplemental figures and tables, which includes Refs. [60,66–75].
- [64] J. P. Perdew, K. Burke, and M. Ernzerhof, *Phys. Rev. Lett.* **77**, 3865 (1996).
- [65] M. Ezawa, *Phys. Rev. B* **89**, 195413 (2014).
- [66] P. E. Blöchl, *Phys. Rev. B* **50**, 17953 (1994).
- [67] V. I. Anisimov, J. Zaanen, and O. K. Andersen, *Phys. Rev. B* **44**, 943 (1991).
- [68] S. Baroni, S. De Gironcoli, A. Dal Corso, and P. Giannozzi, *Rev. Mod. Phys.* **73**, 515 (2001).
- [69] A. A. Mostofi, J. R. Yates, Y.-S. Lee, I. Souza, D. Vanderbilt, and N. Marzari, *Comput. Phys. Commun.* **178**, 685 (2008).
- [70] H. Peng, Z.-H. Yang, J. P. Perdew, and J. Sun, *Phys. Rev. X* **6**, 041005 (2016).
- [71] C. W. Groth, M. Wimmer, A. R. Akhmerov, and X. Waintal, *New J. Phys.* **16**, 063065 (2014).
- [72] S. Zhao, Z. Li, and J. Yang, *J. Am. Chem. Soc.* **136**, 13313 (2014).
- [73] S. Guan, Y. Liu, Z.-M. Yu, S.-S. Wang, Y. Yao, and S. A. Yang, *Phys. Rev. Mater.* **1**, 054003 (2017).
- [74] D. Domaretskiy, M. Philippi, M. Gibertini, N. Ubrig, I. Gutiérrez-Lezama, and A. F. Morpurgo, *Nat. Nanotechnol.* **17**, 1078 (2022).
- [75] Y. Gao, Y. Zhang, and D. Xiao, *Phys. Rev. Lett.* **124**, 077401 (2020).